

Unraveling The Impacts of Meteorological and Anthropogenic Changes on Sediment Fluxes Along an Estuary-Sea Continuum

Florent Grasso (✉ florent.grasso@ifremer.fr)

Ifremer – DYNECO/DHYSED

Eliott Bismuth

Ifremer – DYNECO/DHYSED

Romarc Verney

Ifremer – DYNECO/DHYSED

Research Article

Keywords: estuary, sediment, changes, human, fluxes, pressures, estuarine, anthropogenic

DOI: <https://doi.org/10.21203/rs.3.rs-677174/v1>

License:  This work is licensed under a Creative Commons Attribution 4.0 International License.

[Read Full License](#)

Unraveling the impacts of meteorological and anthropogenic changes on sediment fluxes along an estuary-sea continuum

Florent Grasso^{1,*}, Elliott Bismuth¹, and Romaric Verney¹

¹Ifremer – DYNECO/DHYSED, Centre de Bretagne, CS 10070, Plouzané, F-29280, France
[*florent.grasso@ifremer.fr](mailto:florent.grasso@ifremer.fr)

ABSTRACT

Sediment fluxes at the estuary-sea interface strongly impact particle matter exchanges between marine and continental sources along the land-sea continuum. However, human activities drive pressures on estuary physical functioning, hence threatening estuarine habitats and their ecosystem services. There is an increasing societal need to better predict the potential trajectories of estuarine sediment fluxes resulting from natural and anthropogenic pressures, but the concomitance of human-induced and meteorological-induced changes makes the responses ambiguous. Therefore, this study explores a 22-year numerical hindcast, experiencing contrasted meteorological conditions and human-induced morphological changes (i.e., estuary deepening and narrowing), in order to disentangle the relative contributions of meteorological and anthropogenic changes on net sediment fluxes between a macrotidal estuary and its adjacent coastal sea. Our results highlight that intense wave events induce fine sediment ($\leq 100 \mu\text{m}$) export to the sea but coarser sediment ($\geq 210 \mu\text{m}$) import within the estuary. Remarkably, moderate to large river flows support mud import within the estuary. Over 25 years, the reduction of intense wave and river flow events reduces fine sediment export to the sea. In addition, the estuary morphological changes due to human activities increase fine sediment import within the estuary, shifting the estuary from an exporting to importing system. We propose a conceptualization of mud flux response to river flow and wave forcing, as well as anthropogenic pressures. It provides valuable insights into particle transfers along the land-sea continuum, contributing to a better understanding of estuarine ecosystem trajectories under global changes.

Introduction

Suspended sediments are vectors of nutrients and pollutants along the land-sea continuum¹. However in tidal estuaries, at the interface between continental freshwaters and coastal seas, sediment may be trapped by the interaction of tide-induced and density-induced processes leading to the formation of estuarine turbidity maxima (ETM)²⁻⁶. Such pools of mainly muddy sediment buffer particulate and dissolved matter exchanges between terrigenous and marine sources, may alter the system morphology and thus potentially disturb these extremely productive habitats⁷⁻¹¹.

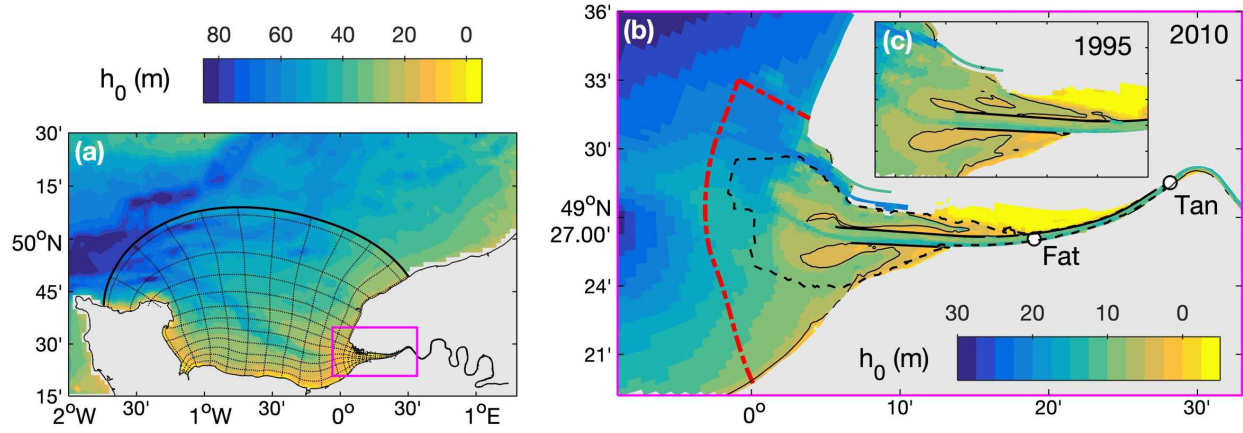
In situ measurements, remote satellite observations, and numerical simulations have shown that estuary sediment fluxes are driven by the combination of hydro-meteorological forcing, such as tide, waves, wind, and river flow¹²⁻¹⁶. Sediment export to coastal seas is usually associated with wave-induced sediment resuspension, whereas sediment import within estuaries mainly results from tidal and gravitational circulations¹⁴. Nonetheless, there is no consensus yet on the phasing of the gravitational circulation contribution concerning the hydrological cycle. For instance, Ganju and Schoellhamer¹⁷ observed a density-induced sediment import within the Suisun Bay (CA, USA) during low river flow, whereas Schulz *et al.*¹⁶ observed that it is enhanced during high river flow in the Seine Estuary (France). Measurements carried out by Sommerfield and Wong¹⁸ in the Delaware Estuary (USA) corroborate Schulz *et al.*'s observations, highlighting that the estuary has

44 a large capacity to buffer extreme river flow and suppress the export of suspended sediment to the
45 Delaware Bay. Nevertheless, it remains difficult to relate sediment fluxes to external forcing due
46 to the general concomitance of antagonist meteorological events, such as stormy (i.e., high waves)
47 and wet (i.e., high river flow) events concurrently occurring during North-Atlantic winter seasons.

48 Net sediment transfers between rivers and seas depend on the estuary hydrological and
49 hydrodynamic regimes, which are modulated by the estuary morphology and the sediment
50 availability¹⁹. Human activities can drastically change the upstream river supplies (e.g., through
51 dam construction²⁰), the local sediment nature (e.g., through dredging activities²¹), and the estuary
52 morphology (e.g., through harbor extension and channelization²²). Guo *et al.*²³ recently
53 investigated a centennial hydro-morphodynamic evolution of the Changjiang Estuary (China) to
54 highlight the influence of anthropogenic pressures on estuary sediment import-export. More
55 specifically, they observed that a narrower funnel-shaped estuary resulting from intensive human
56 activities induced a shift from ebb to flow dominated estuary, leading to increase sediment import
57 and channel aggradation. Such behavior was observed as well in estuaries following severe channel
58 deepening, shifting systems from normal to hyper-turbid states ^{24,25}. However, despite human
59 activities (e.g., dredging), some estuaries can keep balanced sediment budgets over hundreds of
60 years, such as the Humber Estuary, UK²⁶. Nonetheless, Townend and Whitehead²⁶ identified that
61 there is a mechanism for the net export of coarse sediment and that fine material can enter and
62 move upstream, driven by secondary circulation and density currents. This fine-grained import was
63 also observed by Sommerfield and Wong¹⁸ and consistent with the conclusions originally put forth
64 by Meade²⁷.

65 In addition to anthropogenic pressures, meteorological changes can induce the evolution of
66 estuarine forcing (e.g., river flow and storminess) and can exacerbate drastic perturbations as
67 extreme events²⁸⁻³¹. Still, it is challenging to disentangle the effects of meteorological and human-
68 induced changes on estuarine sediment transfers over decades because they concomitantly impact
69 the system's functioning. It is however critical for better understanding and predicting particulate
70 transfers along the land-sea continuum in the context of global changes. Therefore, this study aims
71 at investigating the relative contributions of estuarine key forcing on net sediment transfers
72 between a macrotidal estuary and its adjacent coastal sea, for contrasted conditions representative
73 of anthropogenic and meteorological changes.

74 The analysis is based on a 22-year numerical hindcast of the Seine Estuary (France) comparing
75 two periods with contrasted human-altered morphologies (1990-2000 and 2005-2015, Figure 1).
76 The influence of meteorological changes on sediment transfers is investigated through a global
77 analysis of mean differences over the two periods, but we do not specifically analyze individual
78 extreme events, as already examined for severe tropical storms^{32,33}. Although sediment import-
79 export can depend on the occurrence between tidal phasing and meteorological forcing¹³, this work
80 focuses on fortnightly tide-averaged fluxes to draw a conceptual pattern of wave-river flow
81 contributions to sediment transfers between estuaries and seas.



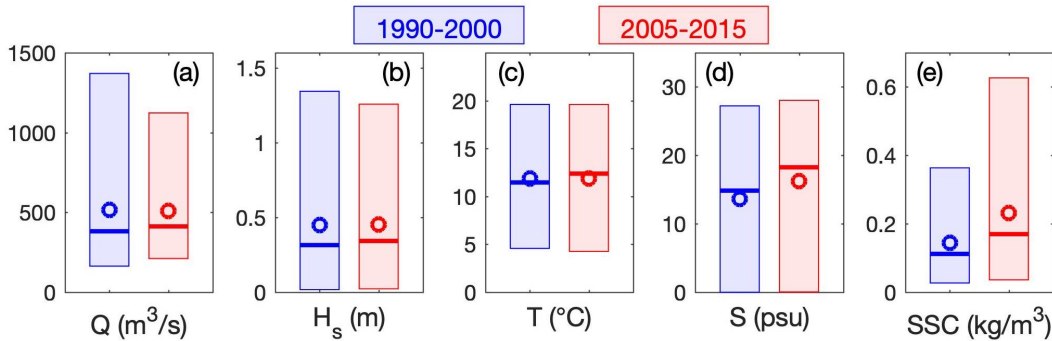
82
 83 **Figure 1.** Bathymetry h_0 of the Seine Estuary, NW France (mean sea level chart datum). (a) Full
 84 model domain with every tenth grid cells represented, (b) focus on the lower estuary in 2010, and
 85 (c) focus on the estuary mouth in 1995. In panels (b,c), solid black contours represent 5-m isobaths,
 86 characterizing intertidal areas. In panel (b), the black dashed contour represents the comparison
 87 area between field surveys and numerical simulations, the red dash-dot line represents the estuary-
 88 sea boundary where sediment fluxes are computed, and the white circles represent Fatouville and
 89 Tancarville locations ('Fat' and 'Tan', respectively).

90 **Results and discussion**

91 **Changes in forcing and environmental parameters**

92 Changes in meteorological forcing during the last decades are analyzed through the median and
 93 extreme values (i.e., 5th, 50th, and 95th percentiles) over the two investigated periods (i.e., 1990-
 94 2000 and 2005-2015), as illustrated in Figure 2. Statistics on the river flow Q are based on the
 95 Seine and its tributaries and statistics on the significant wave height H_s are computed at the estuary-
 96 sea boundary (red dash-dot line in Figure 1b). River flow and wave forcing present similar trends
 97 with an increase of median values (p_{50} : +8% and +9%, respectively) and a decrease of the extreme
 98 values (p_{95} : -18% and -6%, respectively). Such changes do not corroborate our view of climate-
 99 induced changes that would increase extreme events and reduce mean river flow²⁸⁻³⁰. However,
 100 these forcing conditions are representative of two contrasted meteorological decades and are not
 101 directly driven by human-induced changes.

102 Figure 2(c-e) illustrates mean changes in dominant environmental parameters – as near-bed
 103 temperature T , salinity S , and suspended sediment concentration SSC – within the central salt
 104 wedge and ETM areas (i.e., at Fatouville in Figure 1b). The median temperature increased by 1 °C
 105 (+8%), whereas the mean temperature only increased by 0.2 °C. These changes are in agreement
 106 with observations of global warming in the English Channel³⁴. The difference between median and
 107 mean values highlights changes in temperature distributions, but it also alerts us on the estimate
 108 sensitivity to statistic computations. The median salinity substantially increased as well (p_{50} :
 109 +3.4 psu, +23%), with a moderate increase of extreme values. These changes mainly result from
 110 the density-induced salinity intrusion enhanced with anthropogenic changes (i.e., channel
 111 deepening, estuary narrowing), as observed by Grasso and Le Hir²². Finally, changes in SSC are
 112 even stronger, both in median and extreme values (p_{50} : +0.06 kg/m³, +52%; p_{95} : +0.26 kg/m³,
 113 +72%). As for salinity, such an increase in SSC is mainly associated with estuary deepening and
 114 narrowing²², which increases tide- and density-induced upstream sediment transport and
 115 potentially shifts systems toward hyper-turbid states^{10,35,36}.



117
 118 **Figure 2.** Comparison of characteristic environmental parameters between 1990-2000 (blue) and
 119 2005-2015 (red): (a) river flow Q , (b) significant wave height H_s at the estuary-sea boundary (red
 120 dash-dot line in Figure 1b), (c-e) near-bed temperature T , salinity S and SSC , respectively, at
 121 Fatouville ('Fat' in Figure 1b). Boxes range from 5th to 95th percentiles; thick lines and circles
 122 represent median and mean values, respectively.

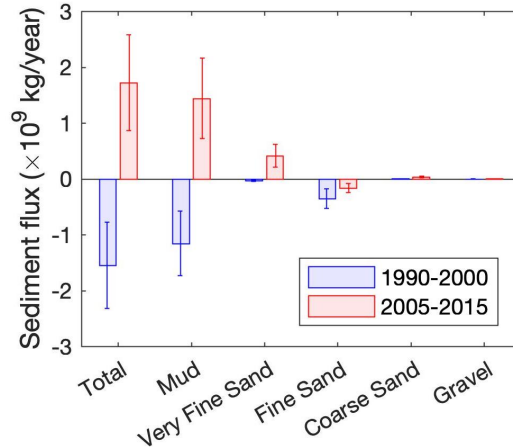
123 Comparison of annual sediment fluxes between 1990-2000 and 2005-2015

124 At the annual time scale, total sediment fluxes present contrasted behaviors along the two periods
 125 (Figure 3), with a net sediment export in 1990-2000 (-1.55×10^9 kg/year) and a net import in 2005-
 126 2015 ($+1.72 \times 10^9$ kg/year). These changes mainly result from the mud dynamics, representing 75%
 127 and 84% of the total fluxes in 1990-2000 and 2005-2015, respectively. The rest of the changes are
 128 attributed to very fine and fine sands, as coarser sediments (i.e., coarse sand and gravel) contribute
 129 to less than 3% of the total fluxes. Note that these coarse sediments ($d > 800 \mu\text{m}$) are mainly
 130 imported within the estuary, in contrast with the Humber Estuary where Townsend and Whitehead²⁶
 131 identified a net export of coarse sediment. Nonetheless, fine sand ($210 \mu\text{m}$) is exported from the
 132 Seine Estuary during the two periods.

133 The shift from total sediment export to import can result from bathymetric changes (estuary
 134 deepening and narrowing; Figure 1b and c), as observed by Guo *et al.*²³. Nonetheless, it may also
 135 result from changes in river flow and wave forcing (Figure 2a and b). Thus, the potential
 136 explanatory factors are further investigated in the following section.

137 Sediment flux response to meteorological forcing

138 To unravel the relative contributions of meteorological forcing (i.e., river flow and wave
 139 conditions) on sediment transfers, sediment fluxes are computed at a shorter time scale. We used a
 140 fortnightly sliding window to average sediment fluxes, river flow, and wave forcing. The 95th
 141 percentiles of river flow and significant wave height are used to represent the forcing parameters
 142 over the fortnightly periods because they showed greater correlations with sediment fluxes rather
 143 than median or mean values. Net fluxes are analyzed through a Q - H_s diagram for the dominant
 144 sediment classes (i.e., mud, very fine and fine sands) and the two periods (Figure 4). Sediment
 145 fluxes are averaged over Q and H_s bins with a spacing of $100 \text{ m}^3/\text{s}$ and 0.1 m , respectively. The
 146 corresponding occurrences (Figure 4c and h) illustrate that the 1990-2000 period experienced
 147 stronger conditions both in river flow and wave forcing than the 2005-2015 period (as observed
 148 in Figure 2a and b).

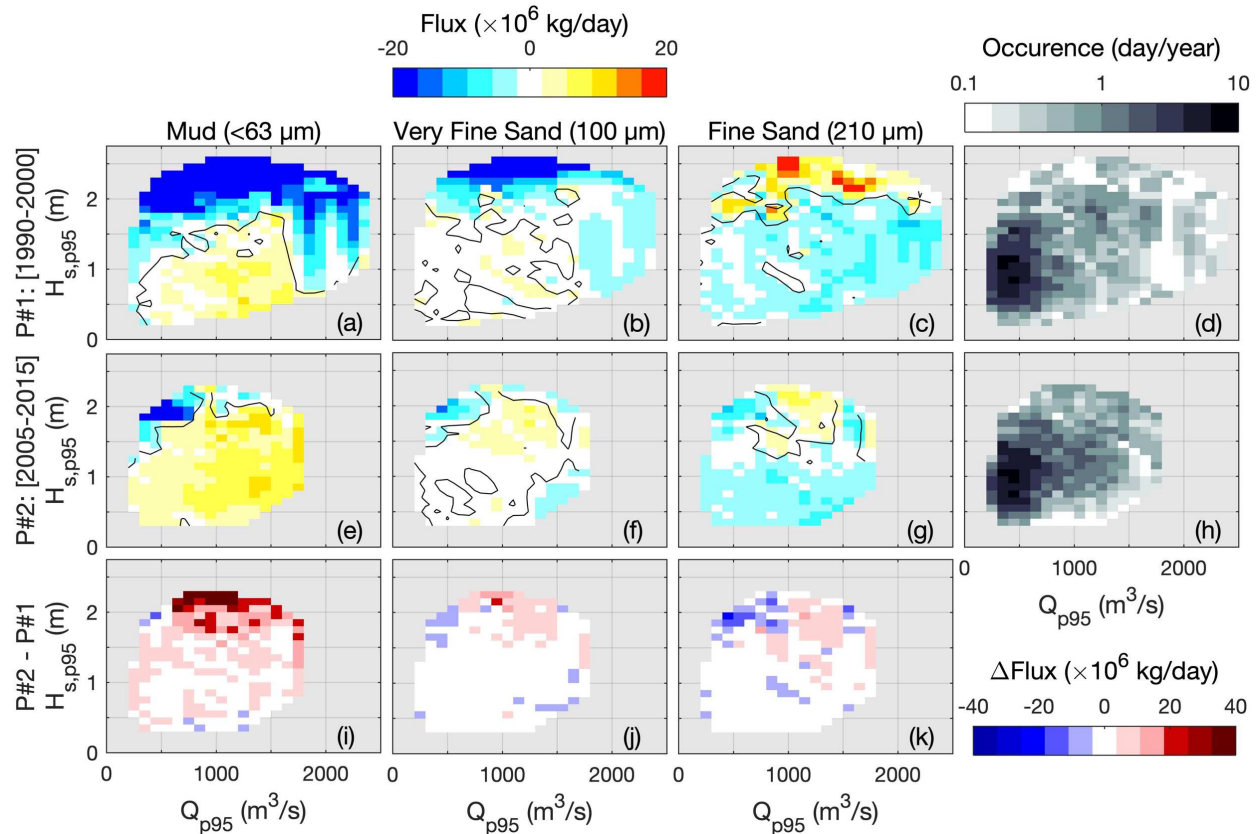


149
 150 **Figure 3.** Comparison of yearly-averaged sediment fluxes at the estuary-sea boundary (red dash-
 151 dot line in Figure 1b) between 1990-2000 (blue) and 2005-2015 (red), for each sediment class and
 152 the sum (Total). Positive fluxes are directed up-estuary (i.e., import) and negative fluxes are
 153 directed seaward (i.e., export). Brackets represent inter-annual standard deviations.

154 In 1990-2000, the mud fluxes present a clear pattern with export increasing with wave
 155 conditions (Figure 4a), resulting from the increase sediment resuspension^{13,14}. Interestingly, the
 156 mud export decreases when river flow increases and even turns out to import for moderate to large
 157 river discharges (i.e., from 400 m³/s to 1500 m³/s). This is characteristic of the enhanced
 158 gravitational circulation observed by Sommerfield and Wong¹⁸ and Schulz *et al.*¹⁶. Nevertheless,
 159 mud fluxes can export again for high river discharges (i.e., >1500 m³/s) when the density-induced
 160 import at the bottom is not sufficiently strong to compensate for the large sediment export at the
 161 surface. In addition, it is remarkable to observe that sands present opposite behaviors depending
 162 on size. There is a tendency to export very fine sand (100 μm), similarly to mud but associated
 163 with weaker fluxes, but import fine sand (210 μm), when wave conditions are the strongest (Figure
 164 4b and c). Such behaviors result from different erodibility thresholds and suspension durations
 165 associated with subtidal currents (i.e., ebb-flow asymmetries in both current intensity and duration;
 166 Nidzioko³⁷). These results point out that different sand classes need to be considered for properly
 167 simulating the diversity of natural sand fluxes and the resulting morphological evolutions.

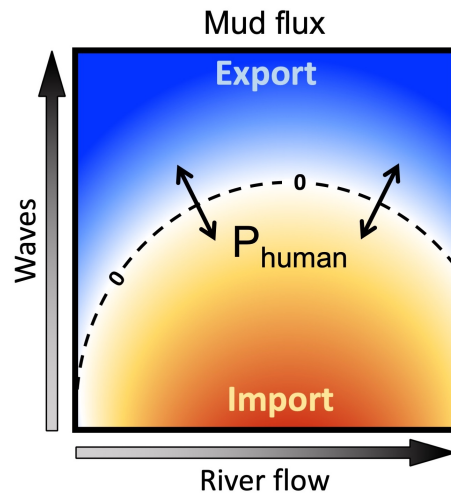
168 Sediment fluxes substantially changed in 2005-2015 with more import of mud and very fine
 169 sand, but less import of fine sand (Figure 4e, f, and g). Such differences can be related to changes
 170 in both meteorological and anthropogenic pressures, which are specifically investigated in the
 171 following section.

172 **Untangling the influences of meteorological and anthropogenic changes on mud fluxes**
 173 Mud fluxes represent more than 75% of the total sediment fluxes between the estuary and the
 174 coastal sea and these very fine particles largely contribute to biogeochemical processes along the
 175 land-sea continuum (e.g., adsorption and desorption mechanisms). Therefore, the present section
 176 focuses on the sensitivity of mud transfers to meteorological and anthropogenic changes. Over the
 177 1990-2000 period, results highlighted that mud export increases with wave forcing, but moderate
 178 to large river discharges support mud import (Figure 4a). This pattern can be schematized through
 179 the $Q-H_s$ diagram in Figure 5. Changes in meteorological conditions between 1990-2000 and 2005-
 180 2015 are observed throughout changes in $Q-H_s$ occurrences (Figure 4d and e). For instance, the
 181 milder conditions experienced in 2005-2015 limit the mud export occurring for large river flow
 182 and wave events, and thus favor mud import within the estuary.



183
 184 **Figure 4.** Comparison of fortnightly-averaged sediment fluxes at the estuary-sea boundary (red
 185 dash-dot line in Figure 1b) between (top panels) the first period P#1 [1990-2000] and (middle
 186 panels) the 2nd period P#2 [2005-2015], in function of the fortnightly-95th percentiles of river flow
 187 (Q_{p95}) and significant wave height ($H_{s,p95}$) forcing, for the three dominant sediment classes (a,e)
 188 mud, (b,f) very fine sand and (c,g) fine sand. Positive fluxes are directed up-estuary (i.e., import)
 189 and negative fluxes are directed seaward (i.e., export). Bottom panels (i-k) represent the flux
 190 differences $\Delta Flux$ between P#2 and P#1. Panels d and h represent the occurrence of $Q-H_s$ forcing
 191 in 1990-2000 and 2005-2015, respectively.

192 Within the same Q and H_s ranges, i.e., for the same meteorological conditions, the mud flux
 193 pattern changes between the two periods (Figure 4a and e). For instance, the isoline delimiting mud
 194 import-export at $Q = 1000 \text{ m}^3/\text{s}$ is close to $H_s = 1.5 \text{ m}$ in 1990-2000 and rises around $H_s = 2 \text{ m}$ in
 195 2005-2015. These changes in mud flux contours are illustrated through the positive flux difference
 196 in Figure 4i (i.e., 2nd period minus 1st period), characterizing more import (or less export) of mud
 197 in 2005-2015 than in 1990-2000. Such a behavior can be attributed to human-induced changes,
 198 which impacted the system functioning via the estuary deepening and narrowing, as observed by
 199 Guo *et al.*²³. Thus, anthropogenic pressures (P_{ant}) would affect the mud pattern schematized in
 200 Figure 5 by shifting the $Q-H_s$ diagram isolines. In other words, the mud fluxes would respond
 201 differently to similar meteorological forcing due to human-induced morphological changes.



202 **Figure 5.** Schematic of mud fluxes in function of river flow and wave forcing. Warm colors
 203 represent up-estuary fluxes (i.e., import) and cool colors represent seaward fluxes (i.e., export).
 204 P_{human} denotes the human-induced pressures impacting the diagram isolines.
 205

206 **Conclusions**

207 A 22-year numerical hindcast (1990-2000 and 2005-2015) of the Seine Estuary sediment dynamics
 208 has been analyzed to investigate the relative contributions of meteorological and anthropogenic
 209 changes on sediment import-export between the estuary and its adjacent coastal sea. From 1990-
 210 2000 to 2005-2015, human pressures induced substantial morphological changes leading to a
 211 deeper and narrower estuary; meteorological conditions (i.e., river flow and wave forcing) changed
 212 with larger median conditions but smaller extreme events. These changes resulted in increasing
 213 salinity intrusion and SSC within the estuary.

214 Net sediment fluxes at the estuary-sea boundary are related to river flow and wave forcing.
 215 Increasing wave conditions enhance the export of very fine sediments ($\leq 100 \mu\text{m}$) and import of
 216 coarser sediments ($\geq 210 \mu\text{m}$). Remarkably, moderate to large river flow conditions support very
 217 fine sediment import. The reduction of extreme conditions in the most recent period (2005-2015)
 218 reduces mud export to the coastal sea. In addition, human-induced morphological changes
 219 perturbed the estuary sediment dynamics and enhanced mud import. Consequently, in less than
 220 25 years, meteorological and anthropogenic changes shifted the estuary from an exporting to an
 221 importing system.

222 The mud flux response to meteorological and anthropogenic changes is schematized through a
 223 “river flow-wave diagram” where meteorological conditions determine the estuary forcing, and
 224 human pressures affect the system's functioning. Such a schematic has to be challenged over other
 225 tidal estuaries. Nevertheless, it represents an excellent tool to investigate potential trajectories in
 226 estuary sediment import-export, directly impacting other compartments of the estuarine ecosystem
 227 (e.g., biogeochemistry, biology, and ecology).

228 **Methods**

229 **Study area**

230 The Seine Estuary (NW France) is a semidiurnal macrotidal system with a tidal range varying from
 231 3 to 8 m at the estuary mouth. It is one of the largest estuaries on the Northwestern European
 232 continental shelf and stretches from the Bay of Seine open to the English Channel to the weir of
 233 Poses upstream, the tidal influence limit (Figure 1). The Seine River flow ranges from 100 to

234 2300 m³/s with a mean annual flow around 450 m³/s and a mean sediment supply around
235 0.7×10⁹ kg/year^{16,38}.

236 The funnel-shaped estuary is exposed to western winds so that the intertidal regions at the mouth
237 are subject to erosion under the combined effect of waves and currents^{39,40}. Waves enter the bay
238 from the northwest with typical significant wave heights of 0.5 m and peaks of more than 3.5 m in
239 front of the estuary mouth. It is characterized by the presence of an ETM that has a pronounced
240 control on the sedimentation patterns of subtidal areas and intertidal mudflats from the estuary
241 mouth up to the upstream freshwater limit, which is few kilometers upstream of Tancarville ('Tan'
242 in Figure 1b)^{6,41-43}.

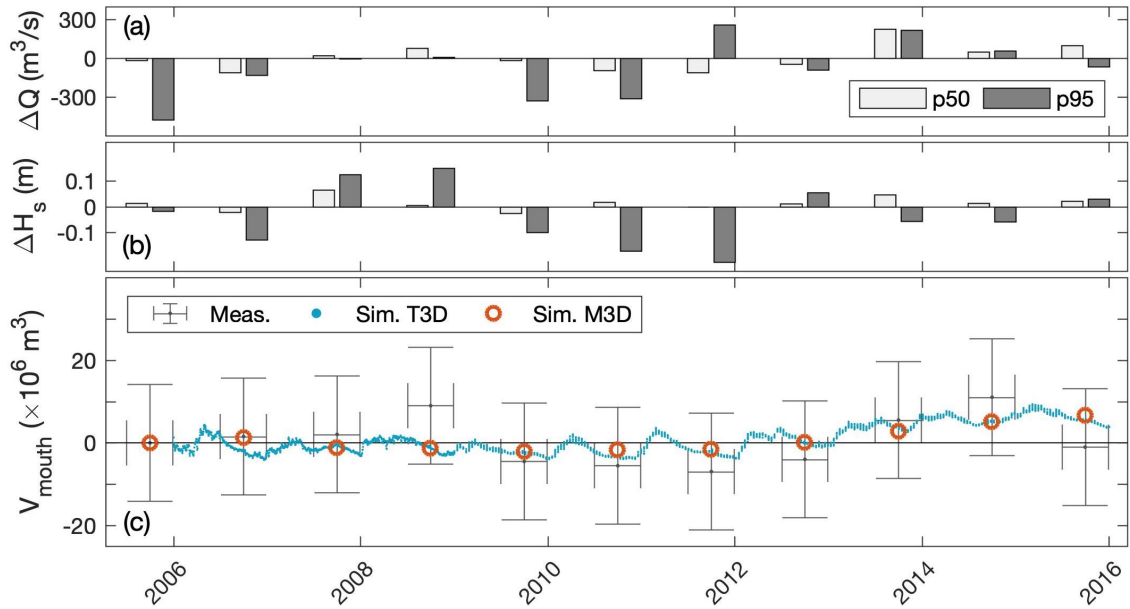
243 During the last century, the Seine Estuary has been vastly altered by human activity⁴¹. As a
244 result, it was changed from a dominantly natural system to a human-controlled system²². In the last
245 decades, i.e., from the 1990s to the 2010s, extensive engineering works induced a deepening and
246 narrowing of the lower estuary. It mainly resulted from the large extension of the Grand Port
247 Maritime du Havre (GPMH) at the estuary mouth (named as "Port 2000") and the main channel
248 deepening and dredging to access the Grand Port Maritime de Rouen (GPMR) approximately
249 120 km upstream of the mouth (Figure 1b and c).

250 Numerical model set-up

251 The ARES hindcast simulations are based on the process-based hydrodynamic and sediment
252 dynamic model developed and validated by Grasso *et al.*⁶. This model has been used by Schulz *et*
253 *al.*¹⁶ to investigate sediment response to idealized hydro-meteorological forcing and by Grasso and
254 Le Hir²² to investigate the influence of contrasted morphologies on ETM dynamics. The model set-
255 up is extensively detailed in the above-mentioned studies; nonetheless, the main model
256 characteristics are reminded hereafter.

257 A non-orthogonal curvilinear mesh extends from the Bay of the Seine to the weir at Poses
258 (Figure 1a) with a resolution around 30×100 m² in the lower estuary (i.e., from the mouth to
259 Tancarville; Figure 1b), corresponding to the main ETM excursion area. The hydrodynamic model
260 is based on the hydrostatic model MARS3D⁴⁴ discretized with 10 equidistant sigma layers. The
261 circulation model is forced by the main tidal components at the sea boundary (CST France,
262 SHOM), the wind stresses and pressure gradients provided by the meteorological ARPEGE model
263 (Meteo-France), and the measured daily discharges from the Seine River and its tributaries. Waves
264 are simulated from the WAVEWATCH III® model⁴⁵ based on a series of embedded computational
265 grids, from a large-scale model of the Atlantic Ocean down to a local model with the same
266 resolution as the circulation model.

267 The hydrodynamic model is coupled with the MUSTANG sediment model for cohesive and
268 non-cohesive mixtures⁴⁶⁻⁴⁸. This multi-layer model accounts for the spatial and temporal variations
269 of sand and mud content in the sediment, as well as for consolidation processes, and resolves
270 advection/diffusion equations for different classes of particles in the water column. This model
271 considers five classes of sediment representative of the Seine Estuary sediment modes⁴⁹: one gravel
272 (diameter $d = 5$ mm), three sands (coarse: $d = 800$ μm, fine: $d = 210$ μm, and very fine:
273 $d = 100$ μm) and one mud. Sediment is initially distributed over a 1-m thick bed according to a
274 realistic bed coverage⁴⁹. The mud advection is calculated using a complete 3D scheme with a
275 variable settling velocity accounting for flocculation processes⁵⁰. The riverine sediment supplies
276 (defined as mud) are imposed at the river flow locations and vary with the freshwater discharges³⁸.
277 In addition, the model simulates the dredging and dumping activities related to the maintenance
278 strategy of the GPMH and GPMR access channels⁶.



279
 280 **Figure 6.** Annual anomalies from 2005 to 2015 of 50th (white) and 95th (gray) percentiles in (a)
 281 river flow ΔQ and (b) significant wave height ΔH_s . (c) Sediment volume V_{mouth} in the estuary mouth
 282 (black dashed contour in Figure 1b), measured from bathymetric surveys (gray brackets), and
 283 simulated from the morphodynamic model TELEMAC3D ‘T3D’ from ARTELIA (blue dots) and
 284 the morphostatic model MARS3D ‘M3D’ used in this study (brown circles).

285 Hindcast simulations over the 1990-2000 and 2005-2015 periods were run through independent
 286 years following a morphostatic approach (i.e., no morphodynamic coupling), which is relevant for
 287 analyzing sediment dynamics at time scales of few years (<5-10 years) when morphological
 288 changes remain relatively small to hydrodynamic processes. The 1995 and 2010 bathymetries were
 289 used to simulate the 1990-2000 and 2005-2015 hindcast, respectively. Each year was run twice to
 290 consider a 1-year spin-up period before analyzing the half-hourly outputs^{6,16,22}. Moreover,
 291 simulations ran from October to October to respect annual hydrological cycles and not to cut down
 292 wet and dry periods.

293 Validation of sediment budgets and fluxes

294 Simulations of sediment transfers between estuaries and coastal seas are prone to large
 295 uncertainties associated with both validation dataset and numerical model parameterization⁵¹.
 296 Grasso *et al.*⁶ validated the Seine Estuary model in terms of hydrodynamics, salinity, and SSC from
 297 tidal to annual time scales at different stations within the estuary. However, Ganju and
 298 Schoellhamer¹⁷ recommend using bathymetric surveys for evaluating the capabilities of a model to
 299 properly reproduce sediment budgets and fluxes. Therefore, the model simulations were compared
 300 to annual bathymetric changes measured in the lower estuary by the GPMR (black dashed contour
 301 in Figure 1b) during the second period (2005-2015, Figure 6c), with regard to annual anomalies of
 302 river flow and wave forcing (Figure 6a and b). The large uncertainties associated with bathymetric
 303 changes are due to both the vertical uncertainties of bathymetric surveys (± 0.1 m) and the
 304 timeframe to cover the entire estuary mouth (~ 6 months). Thus, these measurements have to be
 305 considered as a qualitative view of sediment volume changes in the estuary mouth. In addition,
 306 these large uncertainties inform us that: (i) errors on “ground-truth” measurements can be very

307 large; and (ii) field measurements are still needed to more accurately assess estuarine
308 morphological changes.

309 The present simulations result from morphostatic modeling, so no bathymetric changes in the
310 hydrodynamic model are computed. However, the bed sediment thickness can change with erosion,
311 deposition, and consolidation processes. Hence, sediment volume changes can be computed from
312 differences in bed thickness over the same area as the GPMR bathymetric surveys. While the
313 simulations do not exactly match the measurements, they prove to be in a good capacity to
314 reproduce the main volume changes observed in the estuary mouth over 11 years.

315 To extend the validation, the simulated volume changes from our MARS3D ‘M3D’ model are
316 compared to volume changes resulting from morphodynamic modeling carried out by ARTELIA,
317 based on the finite element TELEMAC3D ‘T3D’ model⁵². T3D continuously simulated ten years,
318 starting from the 2006 bathymetry and with bathymetric adjustment via morphodynamics coupling,
319 whereas M3D simulated 11 independent years considering the 2010 bathymetry. The interest in
320 such a model intercomparison is twofold: (i) both models present very similar results although
321 hydrodynamics and sediment dynamics are differently parameterized and resolved, which provides
322 confidence in the simulation reliability; and (ii) the morphostatic modeling ‘M3D’ used in this
323 study is shown to be relevant for investigating sediment volume changes up to 5 years around a
324 given bathymetry.

325 The capacity to properly simulate changes in sediment volumes provides confidence in the
326 ability to simulate sediment budgets and fluxes. However, changes in sediment volumes do not
327 exactly correspond to changes in sediment mass. For instance, consolidation processes induce a
328 decrease in sediment volume (i.e., sediment compaction), but the sediment mass does not change⁴⁷.
329 Moreover, changes in sediment porosity due to changes in mud-sand mixtures affect the bed
330 volume and not the mass⁵³. Thus, while bathymetric surveys are limited to analyze sediment
331 budgets and fluxes, simulations provide adapted knowledge as changes in sediment mass are
332 explicitly computed.

333 Sediment flux computation

334 The net sediment fluxes are computed at the estuary-sea boundary (red dash-dot line in Figure 1b),
335 in agreement with the ‘offshore’ boundary used by Schulz *et al.*¹⁶. It represents a suitable limit
336 beyond which seaside morphological changes are small compared to estuarine changes^{16,22} and
337 properly characterizing sediment transfers between the estuary and the bay. The fluxes $F_{i,\Delta t}$ during
338 a period Δt are computed for each sediment class i as the difference in sediment mass M_i (i.e.,
339 sediment budget) in the lower estuary area, which is defined between the estuary-sea boundary and
340 Tancarville (Figure 1b), and considering the incoming sediment fluxes at Tancarville $F_{i,Tan}$:

$$341 \quad F_{i,\Delta t} = \Delta M_{i,\Delta t} + \int_0^{\Delta t} F_{i,Tan} dt \quad (1)$$

342 with a positive flux oriented up-estuary (i.e., import) and a negative flux oriented seaward (i.e.,
343 export). $F_{i,Tan}$ is integrated online at every time step across the channel section¹⁶ and M_i is the sum
344 of sediment masses in both water and bed compartments.

345 References

- 346 1 Billen, G. *et al.* A long-term view of nutrient transfers through the Seine river continuum. *Sci Total Environ*
347 **375**, 80-97, doi:10.1016/j.scitotenv.2006.12.005 (2007).
- 348 2 Burchard, H., Schuttelaars, H. & Ralston, D. Sediment Trapping in Estuaries. *Annual review of marine*
349 *science* **10**, 371-395 (2018).
- 350 3 Allen, G. P., Salomon, J., Bassoullet, P., Du Penhoat, Y. & De Grandpre, C. Effects of tides on mixing and
351 suspended sediment transport in macrotidal estuaries. *Sedimentary Geology* **26**, 69-90 (1980).
- 352 4 Scully, M. E. & Friedrichs, C. T. Sediment pumping by tidal asymmetry in a partially mixed estuary.
353 *Journal of Geophysical Research: Oceans* **112** (2007).

354 5 Talke, S. A., de Swart, H. E. & Schuttelaars, H. Feedback between residual circulations and sediment
355 distribution in highly turbid estuaries: an analytical model. *Continental Shelf Research* **29**, 119-135 (2009).

356 6 Grasso, F. *et al.* Suspended Sediment Dynamics in the Macrotidal Seine Estuary (France): 1. Numerical
357 Modeling of Turbidity Maximum Dynamics. *Journal of Geophysical Research: Oceans* **123**, 558-577,
358 doi:10.1002/2017JC013185 (2018).

359 7 Morris, A., Mantoura, R., Bale, A. & Howland, R. Very low salinity regions of estuaries: important sites for
360 chemical and biological reactions. *Nature* **274**, 678-680 (1978).

361 8 Costanza, R. *et al.* The value of the world's ecosystem services and natural capital. *nature* **387**, 253-260
362 (1997).

363 9 Chen, Y. *et al.* Land claim and loss of tidal flats in the Yangtze Estuary. *Scientific Reports* **6**, 1-10 (2016).

364 10 Cox, T., Maris, T., Van Engeland, T., Soetaert, K. & Meire, P. Critical transitions in suspended sediment
365 dynamics in a temperate meso-tidal estuary. *Scientific reports* **9**, 1-10 (2019).

366 11 Donázar-Aramendía, I. *et al.* Human pressures on two estuaries of the Iberian Peninsula are reflected in
367 food web structure. *Scientific reports* **9**, 1-10 (2019).

368 12 Constantin, S., Doxaran, D., Derkacheva, A., Novoa, S. & Lavigne, H. Multi-temporal dynamics of
369 suspended particulate matter in a macro-tidal river Plume (the Gironde) as observed by satellite data.
370 *Estuarine, Coastal and Shelf Science* **202**, 172-184 (2018).

371 13 Geyer, W. R., Woodruff, J. D. & Traykovski, P. Sediment transport and trapping in the Hudson River
372 estuary. *Estuaries* **24**, 670-679 (2001).

373 14 French, J., Burningham, H. & Benson, T. Tidal and meteorological forcing of suspended sediment flux in a
374 muddy mesotidal estuary. *Estuaries and Coasts* **31**, 843-859 (2008).

375 15 Figueroa, S. M. *et al.* Evaluation of along-channel sediment flux gradients in an anthropocene estuary with
376 an estuarine dam. *Marine Geology* **429**, 106318 (2020).

377 16 Schulz, E., Grasso, F., Le Hir, P., Verney, R. & Thouvenin, B. Suspended Sediment Dynamics in the
378 Macrotidal Seine Estuary (France): 2. Numerical Modeling of Sediment Fluxes and Budgets Under Typical
379 Hydrological and Meteorological Conditions. *Journal of Geophysical Research: Oceans* **123**, 578-600,
380 doi:10.1002/2016JC012638 (2018).

381 17 Ganju, N. K. & Schoellhamer, D. H. Calibration of an estuarine sediment transport model to sediment
382 fluxes as an intermediate step for simulation of geomorphic evolution. *Continental Shelf Research* **29**, 148-
383 158 (2009).

384 18 Sommerfield, C. K. & Wong, K. C. Mechanisms of sediment flux and turbidity maintenance in the
385 Delaware Estuary. *Journal of Geophysical Research-Oceans* **116**, doi:Artn C01005
386 10.1029/2010jc006462 (2011).

387 19 Yu, X., Zhang, W. & Hoitink, A. Impact of river discharge seasonality change on tidal duration asymmetry
388 in the Yangtze River Estuary. *Scientific reports* **10**, 1-17 (2020).

389 20 Chu, Z. *et al.* A quantitative assessment of human impacts on decrease in sediment flux from major Chinese
390 rivers entering the western Pacific Ocean. *Geophysical Research Letters* **36** (2009).

391 21 Van Maren, D., Van Kessel, T., Cronin, K. & Sittoni, L. The impact of channel deepening and dredging on
392 estuarine sediment concentration. *Continental Shelf Research* **95**, 1-14 (2015).

393 22 Grasso, F. & Le Hir, P. Influence of morphological changes on suspended sediment dynamics in a
394 macrotidal estuary: diachronic analysis in the Seine Estuary (France) from 1960 to 2010. *Ocean Dynamics*
395 **69**, 83-100 (2019).

396 23 Guo, L. *et al.* A historical review of sediment export–import shift in the North Branch of Changjiang
397 Estuary. *Earth Surface Processes and Landforms* **n/a**, doi:<https://doi.org/10.1002/esp.5084> (2021).

398 24 Winterwerp, J. C. & Wang, Z. B. Man-induced regime shifts in small estuaries—I: theory. *Ocean Dynamics*
399 **63**, 1279-1292 (2013).

400 25 Winterwerp, J. C., Wang, Z. B., van Braeckel, A., van Holland, G. & Kösters, F. Man-induced regime shifts
401 in small estuaries—II: a comparison of rivers. *Ocean Dynamics* **63**, 1293-1306 (2013).

402 26 Townend, I. & Whitehead, P. A preliminary net sediment budget for the Humber Estuary. *Science of the*
403 *total environment* **314**, 755-767 (2003).

404 27 Meade, R. H. Landward transport of bottom sediments in estuaries of the Atlantic coastal plain. *Journal of*
405 *Sedimentary Research* **39**, 222-234 (1969).

406 28 Pachauri, R. K. *et al.* *Climate change 2014: synthesis report. Contribution of Working Groups I, II and III*
407 *to the fifth assessment report of the Intergovernmental Panel on Climate Change.* (Ippc, 2014).

408 29 Young, I. R. & Ribal, A. Multiplatform evaluation of global trends in wind speed and wave height. *Science*
409 **364**, 548-552 (2019).

- 410 30 Passeri, D. L. *et al.* The roles of storminess and sea level rise in decadal barrier island evolution.
411 *Geophysical Research Letters* **47**, e2020GL089370 (2020).
- 412 31 Paerl, R. W., Venezia, R. E., Sanchez, J. J. & Paerl, H. W. Picophytoplankton dynamics in a large temperate
413 estuary and impacts of extreme storm events. *Scientific reports* **10**, 1-15 (2020).
- 414 32 Ralston, D. K., Yellen, B., Woodruff, J. D. & Fernald, S. Turbidity hysteresis in an estuary and tidal river
415 following an extreme discharge event. *Geophysical Research Letters* **47**, e2020GL088005 (2020).
- 416 33 Ralston, D. K., Warner, J. C., Geyer, W. R. & Wall, G. R. Sediment transport due to extreme events: The
417 Hudson River estuary after tropical storms Irene and Lee. *Geophysical Research Letters* **40**, 5451-5455
418 (2013).
- 419 34 Saulquin, B. & Gohin, F. Mean seasonal cycle and evolution of the sea surface temperature from satellite
420 and in situ data in the English Channel for the period 1986–2006. *International Journal of Remote Sensing*
421 **31**, 4069-4093 (2010).
- 422 35 Van Maren, D., Winterwerp, J. & Vroom, J. Fine sediment transport into the hyper-turbid lower Ems River:
423 the role of channel deepening and sediment-induced drag reduction. *Ocean Dynamics* **65**, 589-605,
424 doi:10.1007/s10236-015-0821-2 (2015).
- 425 36 Winterwerp, J. C. Fine sediment transport by tidal asymmetry in the high-concentrated Ems River:
426 indications for a regime shift in response to channel deepening. *Ocean Dynamics* **61**, 203-215 (2011).
- 427 37 Nidzieko, N. J. Tidal asymmetry in estuaries with mixed semidiurnal/diurnal tides. *Journal of Geophysical*
428 *Research: Oceans* **115** (2010).
- 429 38 Landemaine, V. *Erosion des sols et transferts sédimentaires sur les bassins versants de l'Ouest du Bassin de*
430 *Paris: analyse, quantification et modélisation à l'échelle pluriannuelle*, University of Rouen, (2016).
- 431 39 Deloffre, J. *et al.* Sedimentation on intertidal mudflats in the lower part of macrotidal estuaries:
432 Sedimentation rhythms and their preservation. *Marine Geology* **241**, 19-32,
433 doi:10.1016/j.margeo.2007.02.011 (2007).
- 434 40 Verney, R., Deloffre, J., Brun-Cottan, J. C. & Lafite, R. The effect of wave-induced turbulence on intertidal
435 mudflats: Impact of boat traffic and wind. *Continental Shelf Research* **27**, 594-612,
436 doi:10.1016/j.csr.2006.10.005 (2007).
- 437 41 Avoine, J., Allen, G., Nichols, M., Salomon, J. & Larssonneur, C. Suspended-sediment transport in the Seine
438 estuary, France: effect of man-made modifications on estuary—shelf sedimentology. *Marine Geology* **40**,
439 119-137 (1981).
- 440 42 Le Hir, P. *et al.* Fine sediment transport and accumulations at the mouth of the Seine estuary (France).
441 *Estuaries* **24**, 950-963 (2001).
- 442 43 Deloffre, J. *et al.* Sedimentary processes on an intertidal mudflat in the upper macrotidal Seine estuary,
443 France. *Estuarine, Coastal and Shelf Science* **64**, 710-720, doi:10.1016/j.ecss.2005.04.004 (2005).
- 444 44 Lazure, P. & Dumas, F. An external–internal mode coupling for a 3D hydrodynamical model for
445 applications at regional scale (MARS). *Advances in Water Resources* **31**, 233-250 (2008).
- 446 45 Roland, A. & Ardhuin, F. On the developments of spectral wave models: numerics and parameterizations
447 for the coastal ocean. *Ocean Dynamics* **64**, 833-846 (2014).
- 448 46 Le Hir, P., Cayocca, F. & Waeles, B. Dynamics of sand and mud mixtures: A multiprocess-based modelling
449 strategy. *Continental Shelf Research* **31**, S135-S149, doi:10.1016/j.csr.2010.12.009 (2011).
- 450 47 Grasso, F., Le Hir, P. & Bassoullet, P. Numerical modelling of mixed-sediment consolidation. *Ocean*
451 *Dynamics* **65**, 607-616 (2015).
- 452 48 Mengual, B., Hir, P., Cayocca, F. & Garlan, T. Modelling Fine Sediment Dynamics: Towards a Common
453 Erosion Law for Fine Sand, Mud and Mixtures. *Water* **9**, 564, doi:10.3390/w9080564 (2017).
- 454 49 Lesourd, S., Lesueur, P., Fisson, C. & Dauvin, J.-C. Sediment evolution in the mouth of the Seine estuary
455 (France): A long-term monitoring during the last 150years. *Comptes Rendus Geoscience* (2015).
- 456 50 Van Leussen, W. *Estuarine macroflocs and their role in fine-grained sediment transport*. (Ministry of
457 Transport, Public Works and Water Management, National Institute for Coastal and Marine Management
458 (RIKZ), 1994).
- 459 51 Diaz, M. *et al.* Modeling Mud and Sand Transfers Between a Macrotidal Estuary and the Continental Shelf:
460 Influence of the Sediment Transport Parameterization. *Journal of Geophysical Research: Oceans* **125**,
461 e2019JC015643 (2020).
- 462 52 De Linares, M., Walther, R., Schaguene, J., Cayrol, C. & Hamm, L. in *13th International Conference on*
463 *Cohesive Sediment Transport Processes (INTERCOH)*, Leuven. 7-11.
- 464 53 Wooster, J. K. *et al.* Sediment supply and relative size distribution effects on fine sediment infiltration into
465 immobile gravels. *Water Resources Research* **44** (2008).

466

467 **Acknowledgments**

468 This study has been carried out in the framework of the ARES project funded by the Seine-Aval 6
469 research program.

470 **Author contributions**

471 F.G., E.B., and R.V. jointly conducted the study. F.G. developed the idea for the study and
472 performed the supervision. E.B. carried out the 22-year numerical hindcast used in this study. F.G.
473 wrote the main part of the manuscript and R.V. provided substantial contributions. All authors read
474 and approved the final manuscript.

475 **Competing interests**

476 The authors declare no competing interests.

477 **Additional information**

478 The ARES hindcast dataset used in this study is available via the following link:
479 <https://doi.org/10.12770/8f5ec053-52c8-4120-b031-4e4b6168ff29>